Molecular Biology of the Cell
Vol. 19, 498–508, February 2008

B-RAF Regulation of Rnd3 Participates in Actin Cytoskeletal and Focal Adhesion Organization

R. Matthew Klein, Laurie S. Spofford, Ethan V. Abel, Arisa Ortiz, and Andrew E. Aplin

Center for Cell Biology and Cancer Research, Albany Medical College, Albany, NY 12208

Submitted September 13, 2007; Revised November 5, 2007; Accepted November 19, 2007
Monitoring Editor: Jean Schwarzbauer

The actin cytoskeleton controls multiple cellular functions, including cell morphology, movement, and growth. Accumulating evidence indicates that oncogenic activation of the mitogen-activated protein kinase kinase/extracellular signal-regulated kinase 1/2 (MEK/ERK1/2) pathway is accompanied by actin cytoskeletal reorganization. However, the signaling events contributing to actin cytoskeleton remodeling mediated by aberrant ERK1/2 activation are largely unknown. Mutant B-RAF is found in a variety of cancers, including melanoma, and it enhances activation of the MEK/ERK1/2 pathway. We show that targeted knockdown of B-RAF with small interfering RNA or pharmacological inhibition of MEK increased actin stress fiber formation and stabilized focal adhesion dynamics in human melanoma cells. These effects were due to stimulation of the Rho/Rho kinase (ROCK)/LIM kinase-2 signaling pathway, cumulating in the inactivation of the actin depolymerizing/severing protein cofilin. The expression of Rnd3, a Rho antagonist, was attenuated after B-RAF knockdown or MEK inhibition, but it was enhanced in melanocytes expressing active B-RAF. Constitutive expression of Rnd3 suppressed the actin cytoskeletal and focal adhesion effects mediated by B-RAF knockdown. Depletion of Rnd3 elevated cofilin phosphorylation and stress fiber formation and reduced cell invasion. Together, our results identify Rnd3 as a regulator of cross talk between the RAF/MEK/ERK and Rho/ROCK signaling pathways, and a key contributor to oncogene-mediated reorganization of the actin cytoskeleton and focal adhesions.

INTRODUCTION

Oncogene-mediated alterations in the actin cytoskeleton and focal adhesions play an important role in promoting tumor cell motility and invasion. A recently identified oncogene is the serine/threonine kinase B-RAF (Davies *et al*., 2002; Wellbrock *et al*., 2004). Mutations in B-RAF have been found in ~70% of melanomas, 35% of thyroid carcinomas, 14% of borderline ovarian cancers, and 11% of colorectal cancers (Davies *et al*., 2002; Rajagopalan *et al*., 2002; Kimura *et al*., 2003). The most common mutation encodes for a glutamic acid substitution (V600E) within the activation loop of B-RAF, resulting in enhanced activation of B-RAF and the mitogen-activated protein kinase kinase/extracellular signal-regulated kinase 1/2 (MEK/ERK1/2) pathway (Davies *et al*., 2002). A higher proportion of B-RAF mutations are present in invasive, vertical growth phase (VGP) tumors (62%) compared with noninvasive radial growth phase tumors (10%) (Dong *et al*., 2003). Furthermore, B-RAF^{V600E} and MEK activity have been shown to be required for melanoma cell invasion in vitro (Huntington *et al*., 2004; Sumimoto *et al*., 2004). However, the mechanisms underlying B-RAF regulation of tumor invasion are incompletely understood.

Rho GTPases are key regulators of the actin cytoskeleton and focal adhesions. RhoA/B/C (hereafter collectively referred to as Rho) enhance actin stress fiber formation via multiple effectors (Ridley and Hall, 1992; Chrzanowska-Wodnicka and Burridge, 1996). One effector pathway involves the serine/threonine kinases, Rho kinase (ROCK)I/II, which increase actin polymerization by inhibiting the actin-severing activity of cofilin via LIM kinases-1/2 (Ohashi *et al*., 2000a). ROCKs also promote myosin-mediated cross-linking of actin filaments through increasing myosin light chain phosphorylation (Kimura *et al*., 1996), although recent studies indicate that ROCKI and ROCKII elicit distinct effects on the actin cytoskeleton (Yoneda *et al*., 2007). Independently of ROCKs, Rho also promotes actin polymerization through binding and activation of the formin protein mDia1 (Watanabe *et al*., 1999). Notably, alterations in the control of Rho GTPases have been linked to cancer (Jaffe and Hall, 2005).

Other Rho GTPase family members counterbalance Rho activity (Aspenstrom *et al*., 2004). In particular, Rnd3/RhoE/Rho8 (referred to as Rnd3) has been shown to antagonize Rho/ROCK signaling and to disrupt actin stress fibers and focal adhesions in fibroblast and epithelial cells (Guasch *et al*., 1998; Nobes *et al*., 1998; Aspenstrom *et al*., 2004; Chardin, 2006). These effects of Rnd3 have been attributed to enhanced activity of p190RhoGAP (Wennerberg *et al*., 2003) and inhibition of ROCKI (Riento *et al*., 2003). The influence of Rnd3 on actin cytoskeletal organization has been implicated in the regulation of cell migration (Guasch *et al*., 1998) and invasion (Gadea *et al*., 2007). In addition, Rnd3 may also play an important role in cell transformation (Hansen *et al*., 2000; Villalonga *et al*., 2004) and ROCK-mediated apoptosis (Ongusaha *et al*., 2006).

In this study, we provide evidence that mutant B-RAF in melanoma cells disrupts actin cytoskeletal organization and focal adhesion dynamics through control of Rho GTPase

This article was published online ahead of print in *MBC in Press* (http://www.molbiolcell.org/cgi/doi/10.1091/mbc.E07–09–0895) on November 28, 2007.

Address correspondence to: A. E. Aplin (aplina@mail.amc.edu).

Abbreviations used: NHEM, normal human epidermal melanocyte; VGP, vertical growth phase.

signaling. These effects were mediated through B-RAF-MEK suppression of the Rho/ROCK/LIM kinase/cofilin pathway and control of Rnd3 expression.

MATERIALS AND METHODS

Cell Culture

Human WM793 and WM115 VGP melanoma cells were kindly provided by Dr. Meenhard Herlyn (Wistar Institute, Philadelphia, PA) (Satyamoorthy *et al.*, 1997). Melanoma cells were cultured in MCDB 153 (Sigma-Aldrich, St. Louis, MO) containing 20% Leibovitz L-15 medium (Mediatech, Herndon, VA), 2% fetal bovine serum (HyClone Laboratories, Logan, UT), 0.2% (wt/vol) sodium bicarbonate (Mediatech), and 5 μg/ml insulin (Sigma-Aldrich) at 37°C with 5% CO_2. Neonatal foreskins were obtained according to Albany Medical College Institutional Review Board procedures. Normal human epidermal melanocytes (NHEMs) were isolated and cultured, as described previously (Conner *et al.*, 2003).

Antibodies and Inhibitors

The following antibodies were used: ROCKI (611136) and ROCKII (610623) were from BD Biosciences (San Jose, CA); phospho-(S3)-cofilin (3311), phospho-ERK1/2 (9106), phospho-MEK1/2 (9121), myc-tag (2276 and 2272), and hemagglutinin (HA)-tag (2367) were from Cell Signaling Technology (Danvers, MA); total cofilin (ACFL02) was from Cytoskeleton (Denver, CO); B-RAF (sc5284), ERK2 (sc154), total MEK1 (sc219), and Rho (sc179, which detects RhoA/B/C) were from Santa Cruz Biotechnology (Santa Cruz, CA); RhoE/Rnd3 (05-723) and phospho-tyrosine (clone 4G10) were from Upstate Biotechnology (Lake Placid, NY); and vinculin (V4505) and Flag-tag (F3165) were from Sigma-Aldrich. In some experiments, cells were treated with the MEK inhibitor U0126 (Cell Signaling Technology) or the ROCK inhibitor Y27632 (Calbiochem, San Diego, CA).

Plasmids, Transfections, and Infections

The following plasmids were used in this study: pRc-CMV-C3 encoding the C3 transferase exotoxin (Sekine *et al.*, 1989; kindly provided by Dr. Jeffrey Settleman, Massachusetts General Hospital, Boston, MA); HA-tagged wild-type and kinase-dead versions of LIM kinase-1 and -2 in pcDNA3 (Sumi *et al.*, 1999; kindly provided by Drs. Toshikazu Nakamura and Tomoyuki Sumi, Biomedical Research Center, Osaka University, Osaka, Japan); myc-tagged nonphosphorylatable S3A cofilin in pcDNA3 (Arber *et al.*, 1998; kindly provided by Dr. Pico Caroni, Friedrich Miescher Institute, Basel, Switzerland); green fluorescent protein (GFP)-vinculin (Balaban *et al.*, 2001; kindly provided by Dr. Benjamin Geiger, Weizmann Institute of Science, Rehovot, Israel); glutathione transferase (GST)-rhotekin Rho binding domain (RBD) (Ren *et al.*, 1999; kindly provided by Dr. Martin Schwartz, University of Virginia, Charlottesville, VA), pFL-mDia1N1 encoding the Rho-binding domain of mDia1 (Watanabe *et al.*, 1999; kindly provided by Dr. Shuh Narumiya, Kyoto University, Kyoto, Japan); and myc-tagged Rnd3 in pRK5-myc (Aspenstrom *et al.*, 2004; kindly provided by Dr. Pontus Aspenström, Uppsala University, Uppsala, Sweden). For transient transfections, cells were grown to 50–60% confluency, and then they were transfected with expression plasmids using TransIT-LT1 reagent (Mirus Bio, Madison, WI) in complete medium, according to manufacturer's instructions. Cells were processed 36 h after the start of the transfection, unless otherwise indicated.

Adenoviral infections were performed as described previously (Bhatt *et al.*, 2005). The delta B-RAF-ER* cDNA in pBabepuro3 was a generous gift from Dr. Martin McMahon (Cancer Research Institute and Department of Cellular and Molecular Pharmacology, UCSF, San Francisco, CA). Delta B-RAF-ER* expresses an N-terminally truncated active form of B-RAF fused to a modified (G525R) estrogen receptor hormone domain (McMahon, 2001). The delta B-RAF-ER* sequence was subcloned into pAdTrack vector, and recombinant adenovirus was generated (Bhatt *et al.*, 2005). NHEMs were infected with either pAdTrack that encodes GFP or pAdTrack delta B-RAF-ER* for 12 h and treated with 1 μM tamoxifen (Sigma-Aldrich) for 18 h.

RNA Interference

B-RAF$^{\#1}$ small interfering RNA (siRNA) to knockdown total B-RAF and B-RAF^{V600E} siRNA designed to target B-RAF harboring the V600E mutation have been described previously (Calipel *et al.*, 2003; Boisvert-Adamo and Aplin, 2006). Two different siRNA duplexes targeting Rnd3 were used: Rnd$^{\#1}$ (CUACAGUGUUUGAGAAUUAUU) and Rnd$^{\#2}$ (GCGGACAGAUGUUAGUACAUU) (Dharmacon RNA Technologies, Lafayette, CO). The nontargeting siControl$^{\#1}$ was also used (Dharmacon RNA Technologies). The siRNAs were transfected into melanoma cells at a final concentration of 25 nM, using Oligofectamine (Invitrogen, Carlsbad, CA). After transfection, cells were cultured for an additional 72 h in complete medium, and then they were processed for further analysis.

Site-directed Mutagenesis

A siRNA-resistant version of B-RAF^{V600E} (B-RAF^{V600E*}) was constructed from pEF-myc-B-RAF^{V600E} donated by Dr. Richard Marais (Institute of Cancer Research, London, United Kingdom) (Davies *et al.*, 2002). pEF-myc-B-RAF^{V600E} was mutated via inverse-polymerase chain reaction (PCR) mutagenesis by using forward primer ATCGCGATCTCAAGAGTAATAATATATTTCTTCAT and reverse primer GGATGATTGACTTGGCGTGTAAGTAA (underlined bases signify silent mutations intended to disrupt siRNA:mRNA interactions). The PCR-generated amplicons were cleaned with GeneClean kit (Qbiogene, Irvine, CA) and treated with PNK (MBI Fermentas, Hanover, MD) following manufacturer's protocol. DNA was treated with T4 DNA ligase (Invitrogen) and used to transform competent DH5α cells. Colonies were screened by complete DNA sequencing to verify proper mutagenesis.

Imaging

Cells on glass coverslips were washed with phosphate-buffered saline (PBS), fixed with 3.7% paraformaldehyde for 20 min, permeabilized with 0.2% Triton X-100 for 5 min, and blocked in 1% bovine serum albumin (BSA)/PBS for 2 h at room temperature. Coverslips were then incubated with primary antibodies diluted 1:200 in 1% BSA/PBS overnight at 4°C. Coverslips were washed three times with PBS before incubation with appropriate Alexa Fluor-conjugated secondary antibodies (Invitrogen), diluted 1:1000; for 1 h at room temperature. In some instances, the coverslips were incubated with tetramethylrhodamine B isothiocyanate (TRITC)-conjugated phalloidin (Sigma-Aldrich) diluted 1:2000 in 1% BSA/PBS for 1 h to visualize F-actin. Coverslips were mounted using Gel/Mount (Biomedia, Foster City, CA). An Olympus BMX-60 microscope equipped with a cooled charge-coupled device (CCD) sensi-camera (Cooke, Auburn Hills, MI) was used to examine samples. Images were acquired using Slidebook software (Intelligent Imaging Innovations, Denver, CO).

The percentage of cells displaying alterations in cytoskeletal organization was determined in cells costained for F-actin and the appropriate epitope-tag. Quantitation was determined from counting at least 200 transfected cells from multiple experiments, and these cells were compared with cells expressing GFP. Focal adhesion numbers and size were quantified using Image-Pro Plus software (Media Cybernetics, Silver Springs, MD). An integrated morphometric analysis was performed on images to select objects of a size range of $0.1 \leq n \leq 100$ μm^2 as focal adhesions based on the anti-vinculin staining.

Focal adhesion turnover was examined using previously described methods (Webb *et al.*, 2004). In brief, subconfluent WM793 cells treated with siRNA for 72 h were transfected with a GFP-vinculin expression plasmid for an additional 24 h. Cells were then imaged using an Olympus BMX-60 inverted microscope. Images were acquired every 2 min over a 20-min interval with a cooled CCD sensi-camera using Image-Pro Plus software. GFP-vinculin containing adhesions were monitored by marking the position of each adhesion at the initial frame and by monitoring its dynamics throughout the experiment.

Cellular Invasion

The polycarbonate filters of transwell cell culture chambers (8-μm pore size; Corning, Lowell, MA) were coated with 50 μl of growth factor-reduced Matrigel (BD Biosciences). Knockdown melanoma cells were added (3×10^4 cells in 100 μl) to the upper chamber in serum-free medium. The lower chamber was filled with normal melanoma growth medium, thereby establishing a soluble gradient of chemoattractants that promoted cellular invasion. The cells were allowed to invade for 24 h at 37°C, at which time the Matrigel and cells associated with the upper surface of the membranes were removed with cotton swabs. Cells that had invaded through the Matrigel were fixed in 3.7% formaldehyde, and nuclei were stained with Hoechst reagent 33342 (Invitrogen). The extent of cell invasion was determined from random fields at 10× magnification and quantified using Image-Pro Plus software.

SDS-Polyacrylamide Gel Electrophoresis and Western Blotting

Cell were lysed and analyzed as described previously (Conner *et al.*, 2003; Boisvert-Adamo and Aplin, 2006). Immunoreactive bands were developed using enhanced chemiluminescence kits (Pierce Chemical, Rockford, IL). Protein bands were detected with a Fluor-S MultiImager (Bio-Rad, Hercules, CA), and band intensity was quantified using Quantity One image analysis (Bio-Rad).

Rho Pull-Down Assays

Cells were washed with ice-cold PBS and lysed in 50 mM Tris, pH 7.2, 1% Triton X-100, 0.5% sodium deoxycholate, 0.1% SDS, 500 mM NaCl, and 10 mM $MgCl_2$, supplemented with protease inhibitors. Cleared cell lysates were incubated with GST-rhotekin RBD (Ren *et al.*, 1999) attached to glutathione-Sepharose at 4°C for 1 h. The beads were washed three times with wash buffer (50 mM Tris, pH 7.2, 1% Triton X-100, 150 mM $NaCl_2$, and 10 mM $MgCl_2$) and

resuspended in Laemmli's sample buffer. Precipitated Rho-GTP was determined by Western blot analysis.

Real-Time Quantitative Reverse Transcription (RT)-PCR

After knockdown, total RNA was extracted using the PURESCRIPT RNA Isolation kit (Gentra Systems, Minneapolis, MN). RNA was reverse transcribed, and the resulting cDNA was used to detect mRNA abundance with primers for actin (forward TACCTCATGAAGATCCTCACC and reverse TTTCGTGGATGCCACAGGAC) and Rnd3 (forward 5′-AATAGAGTTGAGCCTGTGGG-3′ and reverse 5′-CTAATGTACTAACATCTGTCCGC-3′). Rnd3 primers give a product of ~230 base pairs, and their specificity was confirmed by melt curve analysis. Reactions were performed using SYBR Green mix and the MyiQ Real-Time PCR detection system (Bio-Rad). Final concentrations of the reaction components were: 50 mM KCl, 20 mM Tris-HCl, pH 8.4, 0.2 mM dATP/dCTP/dGTP/dTTP, 25 U/ml DNA polymerase, 3 mM $MgCl_2$, and 200 nM forward and reverse primers. Reaction conditions were denaturation at 94°C for 30 s, annealing at 50°C for 30 s, and elongation at 72°C for 30 s; 40 cycles in total. Relative mRNA levels were calculated using the comparative C_t method (ΔC_t) (Pfaffl, 2001).

RESULTS

Mutant B-RAF Disrupts the Actin Cytoskeleton in Melanoma Cells

B-RAF depletion in WM793 cells, a human VGP melanoma cell line harboring a constitutive active B-RAF^{V600E} allele, with siRNA targeting either total B-RAF (B-RAF$^{\#1}$) or B-RAF^{V600E} (B-RAF^{V600E}) decreased expression of B-RAF and phosphorylation of its downstream targets, MEK and ERK1/2 (Figure 1A). Knockdown was selective because no effect was observed on either C-RAF or A-RAF (Boisvert-Adamo and Aplin, 2006). B-RAF knockdown WM793 cells were less refractive and displayed increased cell area by an average of 39.6% (Supplemental Figure S1, A and B) (Hingorani *et al.*, 2003). These observations prompted us to investigate the role of B-RAF in regulating the actin cytoskeleton in melanoma cells.

F-actin organization was determined in control and B-RAF knockdown cells by fluorescent microscopy. In control WM793 cells, F-actin structures were formed around the periphery of the cells with a few thin stress fibers located within the cell body (Figure 1B). By contrast, B-RAF knockdown in WM793 cells with either of the two B-RAF targeting siRNAs displayed enhanced levels of actin stress fibers, which traversed the cell body (Figure 1B). To address the specificity of B-RAF knockdowns, we mutated the human B-RAF^{V600E} cDNA to introduce four base changes within the B-RAF$^{\#1}$ siRNA target site without altering the amino acid sequence, thereby allowing for expression of B-RAF^{V600E} in melanoma cells treated with B-RAF$^{\#1}$ siRNA. The activity of this siRNA-resistant B-RAF (B-RAF^{V600E*}) was comparable with the nonmutagenized B-RAF^{V600E}, as measured by its ability to phosphorylate MEK1 in COS-7 cell cotransfection experiments (Supplemental Figure S2). Expression of siRNA-resistant B-RAF^{V600E*} in B-RAF$^{\#1}$ knockdown WM793 cells led to the disruption of actin stress fiber organization in 74% of cells (Figure 1C). In control experiments, expression of GFP prevented B-RAF knockdown-induced actin stress fiber formation in only 7% of cells (Figure 1C). To ensure the effects of B-RAF knockdown on the actin cytoskeleton were applicable to more than one cell line, we performed similar experiments in WM115 cells, a VGP cell line that expresses the activating B-RAF^{V600D} mutation (Davies *et al.*, 2002). Overall, the F-actin content seemed to be less structured in control WM115 cells compared with the WM793 cells. Importantly, B-RAF knockdown enhanced actin stress fiber formation in WM115 cells (Figure 1D and Supplemental Figure S3). In summary, these results show that mutant B-RAF regulates the actin cytoskeletal organization in melanoma cells.

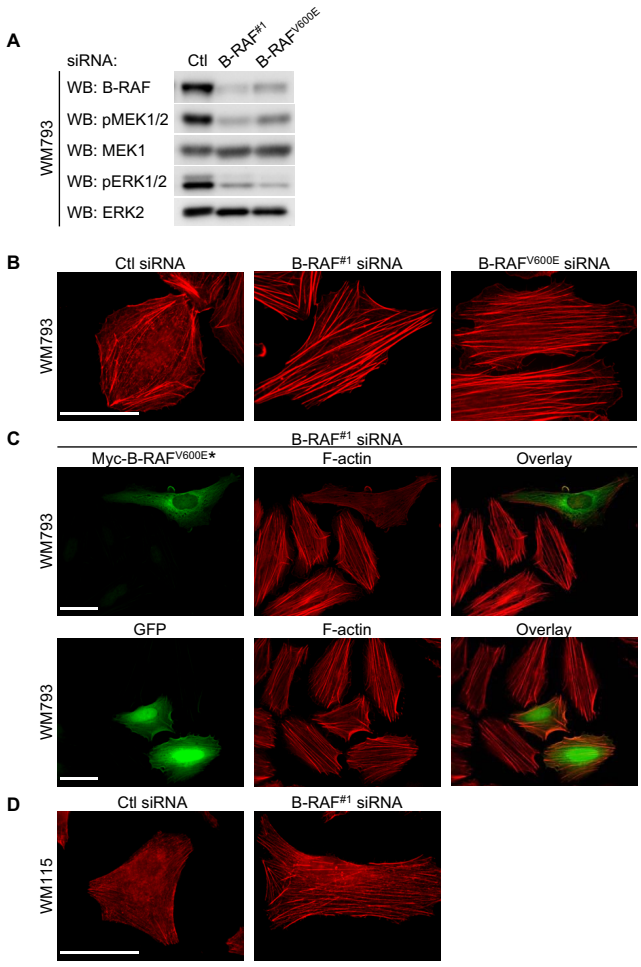

Figure 1. B-RAF knockdown enhances actin stress fiber formation. WM793 cells were transfected with control, total B-RAF (B-RAF$^{\#1}$), or mutant B-RAF (B-RAF^{V600E}) siRNA. (A) Cell lysates were analyzed by Western blotting for B-RAF, phospho-MEK1/2, MEK1, phospho-ERK1/2, and ERK2. (B) F-actin organization was visualized using TRITC-conjugated phalloidin. (C) B-RAF$^{\#1}$ siRNA knockdown WM793 cells were transfected with a myc-tagged mutant B-RAF^{V600E*} that is resistant to duplex #1. Fixed cells were costained with TRITC-phalloidin and anti-myc antibody. Myc-tag staining was visualized using Alexa Fluor 488-conjugated anti-mouse secondary antibodies. Bottom, B-RAF$^{\#1}$ siRNA knockdown WM793 cells were transfected with GFP and stained for F-actin. (D) Vertical growth phase WM115 cells that harbor a B-RAF^{V600D} mutation were transfected with control or B-RAF$^{\#1}$ siRNA and stained for F-actin, as described above. Bars, 50 μm.

The effects of B-RAF knockdown could possibly be attributed to cell cycle arrest because B-RAF knockdown inhibits cyclin D1 expression and G1-S cell cycle progression (Hingorani *et al.*, 2003; Sharma *et al.*, 2005; Bhatt *et al.*, 2007). However, knockdown of cyclin D1, which efficiently inhibits G1-S cell cycle progression in WM793 cells (Bhatt *et al.*, 2005), failed to promote actin stress fiber formation (Supplemental Figure S4). This provides evidence that B-RAF effects on the actin cytoskeleton are not mediated by cyclin D1-dependent downstream actions.

B-RAF Knockdown Regulates Focal Adhesions Dynamics

Focal adhesions mediate integrin-attachment to the extracellular matrix, anchor actin stress fibers, and modulate

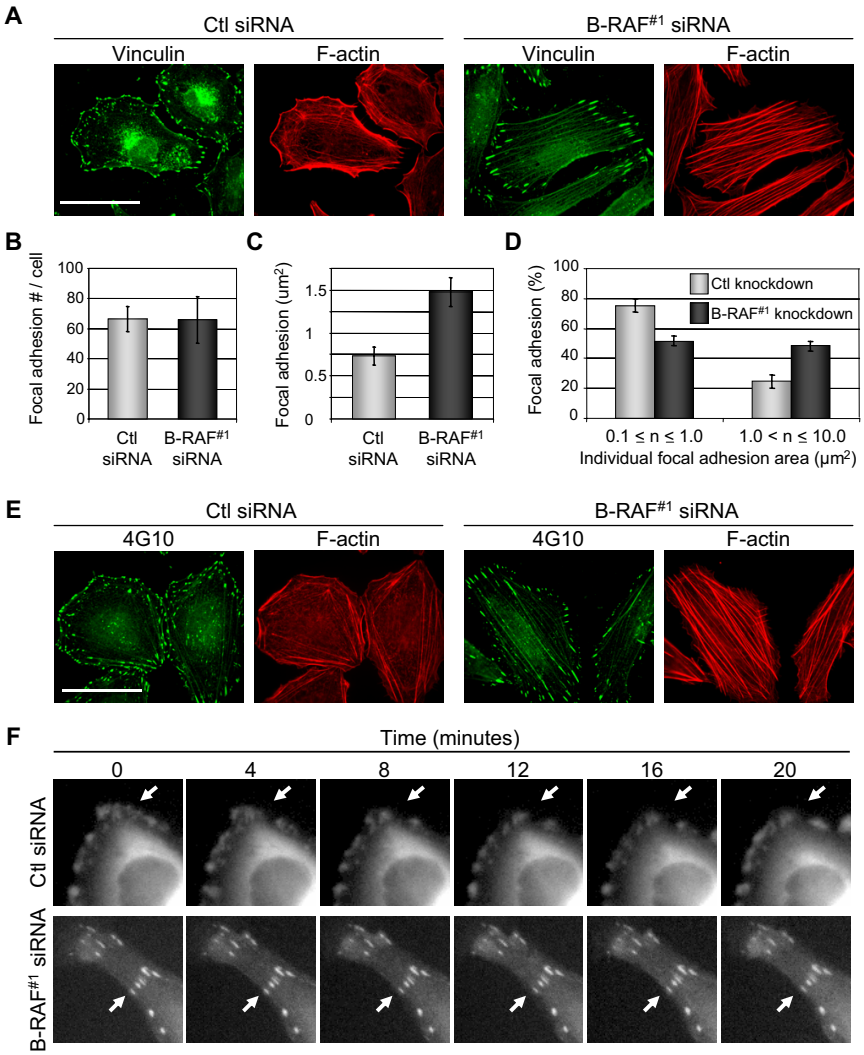

Figure 2. B-RAF influences focal adhesion morphology and dynamics. WM793 cells were transfected with control or B-RAF$^{\#1}$ siRNA for 72 h. Subsequently, cells were fixed and processed for indirect immunofluorescence by staining with vinculin and Alexa Fluor 488-conjugated anti-mouse antibodies. F-actin was visualized by staining with TRITC-phalloidin. Bars, 50 μm. (B) The number of vinculin-staining focal adhesions was quantitated from control and B-RAF knockdown WM793 cells using Image-Pro Plus software. Five cells were analyzed per condition in each experiment. Three independent experiments were performed. (C) The average size of vinculin-containing focal adhesions was quantitated from control and B-RAF knockdown WM793 cells. (D) The number of small (0.1–1.0 μm^2) and large (>1.0 μm^2) focal adhesions was quantitated from control and B-RAF knockdown WM793 cells. (E) As described in A, except that anti-phosphotyrosine antibodies were used. (F) WM793 cells expressing GFP-vinculin were treated with control or B-RAF$^{\#1}$ siRNA. Fluorescence images taken after 0, 4, 8, 12, 16, and 20 min are shown. Arrows indicate examples of GFP-vinculin–containing adhesions that either undergo rearrangement (top) or do not change (bottom).

cell migratory behavior. We next determined whether B-RAF regulated focal adhesion organization. Control and B-RAF knockdown WM793 cells were stained for vinculin, a component of focal adhesions. Control knockdown cells displayed small punctate focal adhesions; by contrast, B-RAF knockdown cells displayed large elongated focal adhesions, which colocalized with the ends of stress fibers (Figure 2A). Quantitation showed no dramatic difference in the numbers of vinculin-staining focal adhesions between control and B-RAF knockdown cells (Figure 2B). However, the average area of focal adhesions and the number of large (>1 μm^2) focal adhesions were increased after B-RAF knockdown (Figure 2, C and D). Focal adhesions are enriched in tyrosine-phosphorylated proteins, and larger focal adhesions were also detected after B-RAF knockdown by immunofluorescence with anti-phosphotyrosine antibodies (Figure 2E).

The formation of larger focal adhesions in B-RAF knockdown cells is suggestive of altered focal adhesion turnover. Hence, we monitored focal adhesion dynamics by examining cells expressing GFP-vinculin. Control and B-RAF knockdown cells were transiently transfected with a GFP-vinculin expression plasmid before acquiring time-lapse images of vinculin-containing focal adhesions. In control siRNA knockdown cells (Figure 2F, top, and Supplemental Figure S5A and S5C), GFP-vinculin formed small focal adhesion structures that frequently assembled, disassembled, and translocated along the cell periphery during the 20-min imaging period. In contrast, B-RAF knockdown cells displayed GFP-vinculin that was incorporated into larger focal adhesions, and its presence in these structures was stable over the time period measured (Figure 2F, bottom, and Supplemental Figure S5B and S5D).

Mutant B-RAF Regulates Rho Activity but Does Not Alter ROCK Expression

Actin stress fiber formation is a characteristic feature of Rho GTPase signaling (Ridley and Hall, 1992); hence, we analyzed Rho GTPase levels by using the rhotekin-RBD pull-down assay. Total levels of Rho did not change after B-RAF knockdown in WM793 cells (Figure 3A), as measured using an antibody that recognizes RhoA/B/C; however, GST-RBD pulled down 3.9-fold more GTP-bound RhoA/B/C from lysates of B-RAF knockdown cells compared with controls (Figure 3, A and B), suggesting enhanced Rho activity.

We next determined whether the effects of B-RAF knockdown on the actin cytoskeleton were dependent on increased Rho activity. Initially, B-RAF knockdown WM793 cells were transfected with a C3 transferase expression construct. C3 transferase is a clostridium botuli-

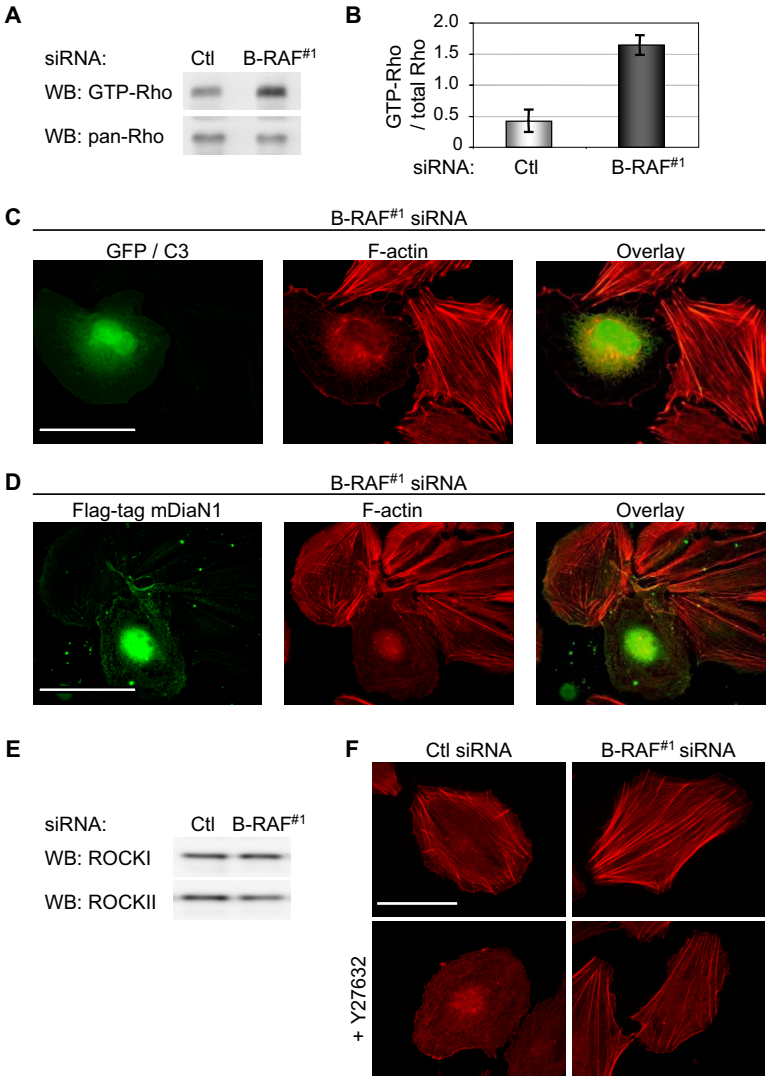

Figure 3. B-RAF controls actin organization via the Rho/ROCK pathway. (A) Activation of Rho in control and B-RAF knockdown cells was measured using the GST-rhotekin pull-down assay. Levels of GTP-bound Rho were determined by Western blot analysis by using a pan-RhoA/B/C antibody. (B) Graphed are the relative amounts of GTP-bound Rho after control or B-RAF$^{\#1}$ knockdown. Each value represents the mean ± SD of three independent experiments. (C) B-RAF knockdown WM793 cells cotransfected with C3 exotoxin and GFP. After 24 h, cells were fixed and processed to visualize F-actin (red) and GFP (green). (D) B-RAF knockdown WM793 cells transfected with Flag-tagged mDia-N1 for 24 h. Cells were then processed to visualize actin organization (red) and Flag-mDiaN1–expressing cells (green). (E) Western blot analysis of ROCKI and ROCKII in control and B-RAF$^{\#1}$ siRNA-treated WM793 cells. (F) F-actin organization in WM793 cells transfected with control and B-RAF$^{\#1}$ siRNA ± treatment with 5 μM Y27632. Bars, 50 μm.

num exoenzyme that ADP-ribosylates and inhibits Rho GTPase activity (Sekine *et al.*, 1989). Expression of C3 transferase in WM793, as determined by cotransfection with GFP, disrupted actin stress fibers in B-RAF knockdown cells (Figure 3C). We also used a construct encoding the Rho binding domain of mDia1 (mDia1N1) that interacts selectively with Rho-GTP, but not Rac1-GTP or Cdc42-GTP, and it blocks GTP-Rho activation of multiple downstream effectors (Watanabe *et al.*, 1999). Similar to expression of C3, mDiaN1 potently inhibited stress fiber formation in B-RAF knockdown WM793 cells (Figure 3D).

The findings that Rho signaling was required for enhanced actin stress fiber formation in B-RAF knockdown cells led to analysis of the Rho effector pathways used. Previous studies have shown that active MEK down-regulates expression of ROCKI and/or ROCKII (Sahai *et al.*, 2001; Pawlak and Helfman, 2002a,b). By Western blot analysis, we did not detect an alteration in the expression level of either ROCKI or ROCKII after B-RAF knockdown (Figure 3E). However, treatment of B-RAF knockdown cells with the ROCK inhibitor Y27632 attenuated actin stress fiber formation (Figure 3F). Together, these data show that signaling through the Rho/ROCK pathway enhances stress fiber formation after B-RAF knockdown. Our data do not rule out the involvement of additional Rho effectors.

LIM Kinase-2 Mediates Enhanced Actin Stress Fibers in B-RAF Knockdown Cells

Major effectors of Rho/ROCK signaling are the LIM kinases-1/2 (Maekawa *et al.*, 1999; Ohashi *et al.*, 2000b; Sumi *et al.*, 2001). To determine whether LIM kinases play a role in melanoma actin organization, we expressed HA-tagged forms of LIM kinase-1 or -2 in WM793 cells, and we analyzed actin stress fiber formation. Ectopic expression of wild-type LIM kinase-2 led to enhanced actin stress fiber formation; whereas LIM kinase-1 elicited moderate effects (Figure 4, A and B). Quantitation showed that 66% of the LIM kinase-1 and 75% of the LIM kinase-2–expressing cells displayed enhanced stress fibers. In control experiments with GFP-expressing cells, only 16% of cells displayed prominent stress fibers (data not shown). Additionally, expression of kinase-dead LIM kinase-2 inhibited stress fiber formation induced by B-RAF knockdown in 67% of cells; whereas kinase-dead LIM kinase-1 only disrupted stress fibers in 17% of cells (Figure 4, C and D). These results suggest that, after B-RAF knockdown, LIM

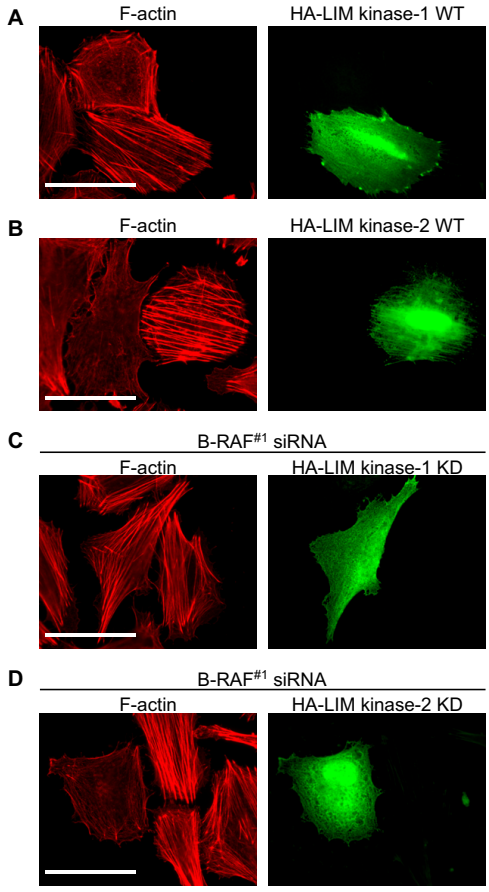

Figure 4. LIM kinase-2 mediates actin stress fiber formation after B-RAF knockdown. WM793 cells were transfected with HA-tagged wild-type (A) LIM kinase-1 or (B) LIM kinase-2. B-RAF knockdown WM793 cells were transfected with either kinase-dead HA-tagged (C) LIM kinase-1 or (D) LIM kinase-2. Cells were fixed and stained to visualize HA-tagged proteins (green) and F-actin organization (red). Bars, 50 μm.

kinase-2 participates in the pathway activated by Rho to affect actin cytoskeletal organization.

Cofilin Phosphorylation Is Regulated by B-RAF

The actin-severing protein cofilin is the principal known LIM kinase substrate (Arber *et al*., 1998; Yang *et al*., 1998). To investigate whether B-RAF signaling alters cofilin activity, we monitored phosphorylation at serine-3, which negatively regulates cofilin activity. B-RAF knockdown WM793 cells showed an average 4.5-fold increase in the level of phospho-cofilin compared with that of control transfectants (Figure 5A). Likewise, B-RAF knockdown in WM115 cells increased cofilin phosphorylation by an average of 3.1-fold (Figure 5B and Supplemental Figure S3). To examine the role of cofilin in melanoma cytoarchitecture, we analyzed the actin organization in B-RAF-depleted WM793 cells cotransfected with a constitutively active myc-tagged cofilin(S3A) mutant. Immunofluorescence staining showed that expression of myc-cofilin(S3A) prevented B-RAF knockdown generation of actin stress fibers (Figure 5C).

We next assessed the involvement of ROCKI/II in B-RAF-mediated cofilin activation by treating cells with a ROCK inhibitor Y27632. Treatment with Y27632 lowered basal phospho-cofilin levels in control knockdown cells, and it moderately suppressed the increase in cofilin phosphorylation accompanying B-RAF knockdown (Figure 5D). This partial effect likely reflects an incomplete inhibition of ROCK activity by Y27632 and/or the involvement of additional Rho effectors. Nevertheless, these data implicate ROCKI/II signaling in B-RAF regulation of cofilin activation.

MEK Signaling Is Required for Actin Cytoskeletal Disruption and Cofilin Activation

Studies show that B-RAF is the main RAF activator of the MEK/ERK1/2 pathway (Huser *et al*., 2001; Mikula *et al*., 2001; Pritchard *et al*., 2004). Treatment of WM793 cells with the pharmacological MEK inhibitor U0126, blocked ERK1/2 phosphorylation (Figure 6A) and it enhanced actin stress fiber formation (Figure 6B). Notably, despite the rapid inhibition of ERK1/2 phosphorylation by U0126, no alteration in actin organization was observed after short-term drug treatment. Rather, prolonged MEK inhibition (>12 h) was required to increase stress fiber formation. Consistent with a role for MEK signaling in the regulation of cofilin activity, treatment with U0126 enhanced cofilin phosphorylation (Figure 6A). Importantly, the kinetics of U0126-induced cofilin phosphorylation correlated with actin stress fiber formation. These data indicate that sustained MEK inactivation is necessary before the formation of stress fibers.

Oncogenic B-RAF Activation of the MEK-ERK1/2 Pathway Increases Rnd3 Expression

Rnd3 is a member of the Rho-family of small GTP-binding proteins that has been implicated in the negative regulation of actin stress fiber formation (Riento *et al*., 2003; Wennerberg *et al*., 2003; Chardin, 2006). Furthermore, Rnd3 has been shown to be regulated by ectopic expression of C-RAF and MEK activity in Madin-Darby canine kidney (MDCK) cells (Hansen *et al*., 2000). We determined whether B-RAF-MEK signaling was necessary for Rnd3 expression in melanoma cells. Incubation of WM793 cells with the MEK inhibitor U0126 resulted in a time-dependent reduction in the level of Rnd3 (Figure 7A). The reduction in Rnd3 levels by U0126 preceded the accompanying increases in cofilin phosphorylation and actin stress fibers (compare Figure 7A and Figure 6, A and B). Expression of Rnd3 was also reduced after knockdown of total B-RAF or B-RAF^{V600E} in WM793 cells (Figure 7B). Similar results were obtained in B-RAF knockdown WM115 cells (Figure 7C and Supplemental Figure S3). Real-time quantitative RT-PCR analysis showed that Rnd3 mRNA abundance was decreased following B-RAF knockdown (Figure 7D), indicating that B-RAF regulates Rnd3 mRNA levels.

To determine whether B-RAF activation is sufficient to induce Rnd3 expression, normal human melanocytes were infected with an adenovirus to express a conditionally activated B-RAF (ΔB-RAF:ER*). Infected cells were cultured for 18 h in the absence or presence of tamoxifen, which enhances expression and activates the fusion protein. As expected, the addition of tamoxifen increased ERK1/2 phosphorylation in ΔB-RAF:ER*-infected melanocytes (Figure 7E). The elevated ERK1/2 phosphorylation in the absence of tamoxifen is probably due to low amounts of agonist within serum or incomplete binding of 90-kDA heat-shock protein to the ΔB-RAF:ER fusion (McMahon, 2001). Western blot analysis showed that expression and activation of ΔB-RAF:ER* was sufficient to induce the expression of Rnd3 in melanocytes and reduce cofilin phosphorylation at serine-3 (Figure 7E). These data show that B-RAF-MEK signaling regulates Rnd3 protein expression in melanocytic cells.

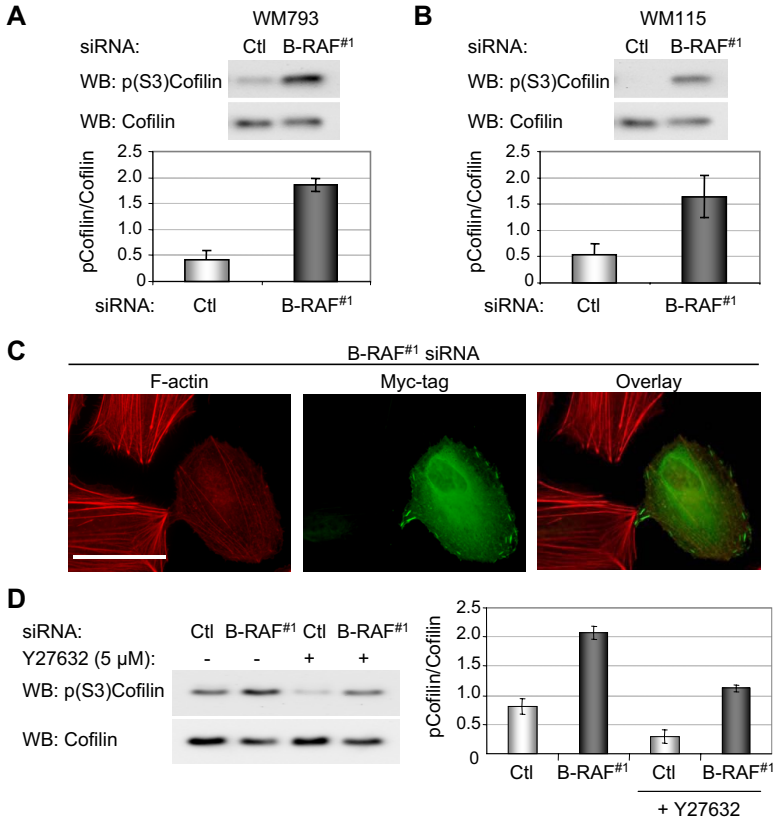

Figure 5. Increased cofilin phosphorylation at serine-3 upon B-RAF knockdown. (A) Western blot analysis of phospho-(S3)-cofilin and total cofilin levels in WM793 cells transfected with control or B-RAF$^{\#1}$ siRNA. The graph represents the relative amounts of phospho-cofilin from three independent experiments. (B) As described in A, except that WM115 cells were analyzed. (C) B-RAF knockdown WM793 cells transfected with myc-tagged active cofilin(S3A). Cells were fixed and processed to visualize F-actin (red) and myc-tagged cofilin (green). Bar, 50 μm. (D) Western blot analysis of phospho-(S3)-cofilin and total cofilin levels in control and B-RAF knockdown WM793 cells treated ± with 5 μM Y27632. The graph represents the phospho-cofilin/total cofilin ratios from two independent experiments.

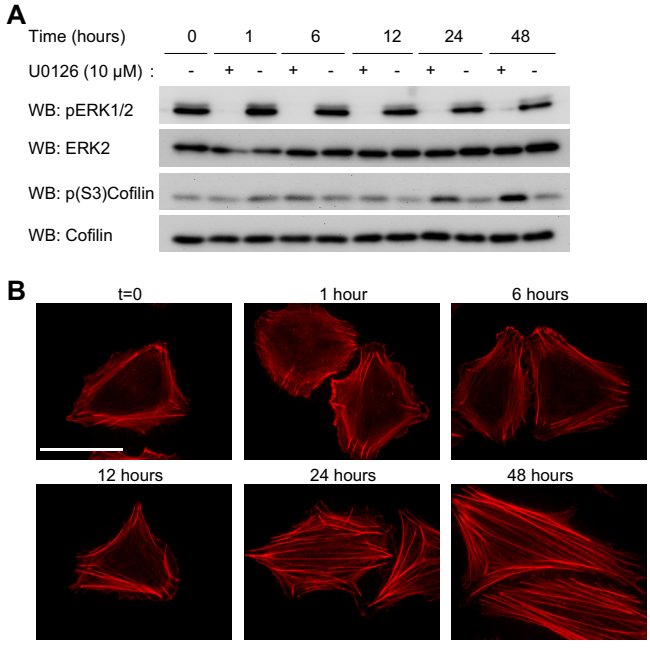

Figure 6. MEK signaling regulates actin stress fibers and cofilin phosphorylation. WM793 cells were incubated with the MEK inhibitor U0126 (10 μM) or an equal volume of dimethyl sulfoxide (DMSO) (−) for 1, 6, 12, 24, and 48 h. (A) Cells lysates generated at the indicated times were analyzed by Western blotting for levels of phospho-ERK1/2, total ERK2, phospho-(S3)-cofilin and total cofilin. Shown are representative blots from three independent experiments. (B) Cells were fixed at indicated times and stained with TRITC-phalloidin to visualize F-actin. Bars, 50 μm.

Rnd3 Regulates Stress Fiber Formation, Focal Adhesion Remodeling, and Invasion

To determine whether Rnd3 participated in mutant B-RAF suppression of stress fibers, we transfected B-RAF knockdown WM793 cells with myc-tagged Rnd3 (Figure 8A) (Aspenstrom *et al.*, 2004). Expression of Rnd3 attenuated the increase in actin stress fiber formation that followed B-RAF knockdown (Figure 8B). Additionally, focal adhesions were more punctate in B-RAF knockdown cells expressing the myc-tagged Rnd3 (Figure 8C).

Finally, we determined the role of endogenous Rnd3 expression in WM793 cells. Depletion of Rnd3 using two different siRNA duplexes resulted in a modest yet consistent increase in cofilin phosphorylation (Figure 9, A and B) and actin stress fiber formation (Figure 9C). Because alterations in the actin cytoskeleton and focal adhesions play an important role in promoting tumor cell invasion, Rnd3 knockdown cells were plated on Matrigel-coated transmembrane filters, and cell invasion was measured. Rnd3 knockdown cells displayed an approximate 40–50% reduction in cell invasion compared with controls (Figure 9D). Together, these observations identify Rnd3 as a downstream target of mutant B-RAF that participates in oncogene-mediated regulation of actin organization and focal adhesion remodeling, and support, at least in part, the acquisition of an invasive phenotype.

DISCUSSION

Oncogenic signaling frequently leads to actin cytoskeletal reorganization; however, the underlying mechanisms are not completely understood. The serine/threonine kinase B-RAF is mutated in ~7% of all cancers (Davies *et al.*, 2002).

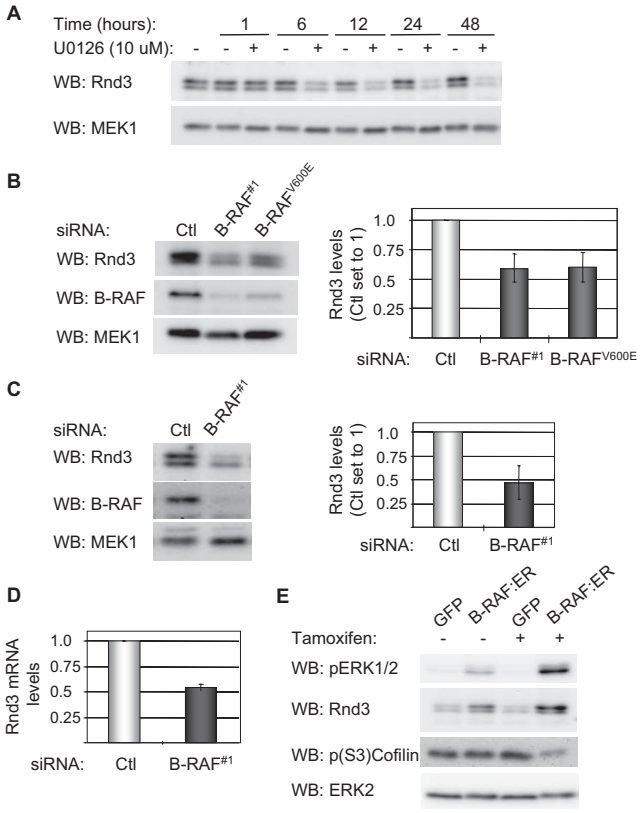

Figure 7. B-RAF and MEK regulate the expression of Rnd3. (A) WM793 cells were treated with 10 μM U0126 or equal volume DMSO for increasing times, as indicated. Cell lysates were western blotted using antibodies to Rnd3 and total MEK, as a loading control. (B) Western blot analysis of Rnd3, B-RAF, and MEK1 levels in WM793 cells transfected with control, B-RAF$^{\#1}$, or B-RAF^{V600E} siRNA. Data are the mean ± SD for the Rnd3/MEK1 ratios from three independent experiments. The control siRNA condition is set to one. (C) Similar to above, except that WM115 cells were transfected with control or B-RAF$^{\#1}$ siRNA. (D) Total RNA was extracted from control and B-RAF knockdown WM793 cells. Quantitative RT-PCR analysis was performed with primers specific for Rnd3 and actin. The graph represents the mean percentage of change in Rnd3 mRNA relative to actin from two independent experiments. (E) NHEM cells infected with adenovirus to express ΔB-RAF:ER* or GFP were incubated 18 h in the absence or presence of tamoxifen. Cell lysates were Western blotted for phospho-ERK1/2, Rnd3, phospho-(S3)-cofilin, and total ERK2.

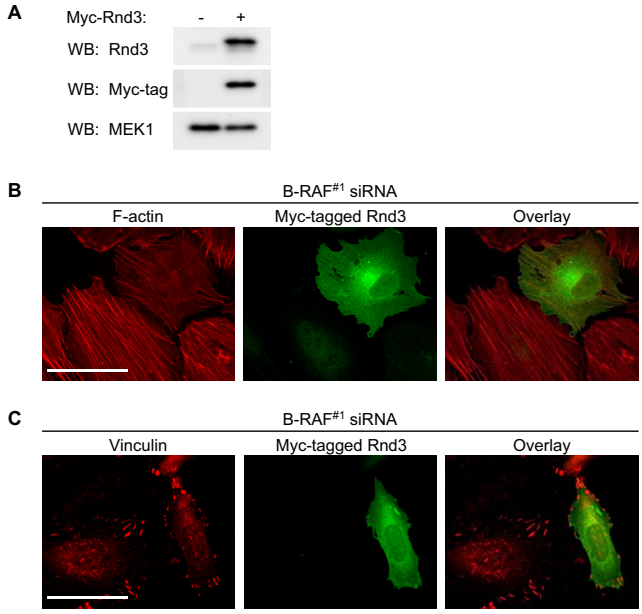

Figure 8. Involvement of Rnd3 in B-RAF knockdown induced stress fiber and focal adhesion formation. WM793 cells were transfected with B-RAF$^{\#1}$ siRNA for 72 h, followed by transfection with cDNA encoding myc-epitope tagged Rnd3. (A) Western blot analysis with Rnd3, myc-tag, and MEK1 antibodies in transfected cell lysates. (B) Cells costained with TRITC-phalloidin (red) and anti-myc antibodies (green). (C) Cells costained with anti-vinculin (red) and anti-myc antibodies (green). Bars, 50 μm.

Here, we demonstrate that mutant B-RAF expression in melanoma cells regulates actin cytoskeletal and focal adhesion organization. Furthermore, B-RAF control of the Rho antagonist Rnd3 contributes to oncogene-mediated reorganization of actin cytoskeleton and focal adhesions.

We initially focused on mutant B-RAF down-regulation of actin stress fiber formation and Rho activity. Our findings are consistent with studies in colon carcinoma cells that demonstrate that constitutive K-RAS signaling via MEK inhibits Rho activation and actin stress fiber formation (Vial *et al*., 2003; Pollock *et al*., 2005). Although Rho activity is reduced in both melanoma and colon carcinoma cells, the molecular mechanisms mediating these changes are distinct. In colon cancer cells, MEK-regulated expression of Fra-1, an AP-1 family member, reduced actin stress fiber formation by inactivating β1 integrins (Vial *et al*., 2003; Pollock *et al*., 2005). Our results suggest a model in which mutant B-RAF promotes melanoma cell invasion at least in part through its control of Rnd3, which inhibits the Rho/ROCK/LIM kinase/cofilin signaling pathway leading to actin stress fiber suppression and focal adhesion turnover (Figure 9E). The combined data reinforce the notion that the MEK/ERK pathway balances Rho activation, although context dependent differences in the mechanism of cross talk may exist.

In contrast to our findings in human melanoma cells, Pritchard *et al*. (2004) have shown that B-RAF$^{-/-}$ mouse embryonic fibroblasts (MEFs) have disorganized actin stress fibers and reduced ROCKII expression. Differences may be due to a transient depletion of B-RAF in our knockdown experiments compared with long-term knockout. Consistent with this notion, we found that knockdown of B-RAF in human foreskin fibroblasts was not associated with discernible changes in actin stress fibers or ROCKII expression (Supplemental Figure S6). Others have shown MEK-dependent alterations in the Rho effectors ROCKI/II disrupt actin stress fiber organization (Sahai *et al*., 2001; Pawlak and Helfman, 2002a; Pawlak and Helfman, 2002b). We found that ROCKI/II expression was not regulated by B-RAF, although ROCK and LIM kinase signaling were required for B-RAF knockdown mediated stress fiber formation. Cofilin is known to be an important contributor to actin organization downstream of ROCK/LIM kinase (Maekawa *et al*., 1999) and its activation has been linked to the formation of cell protrusions (Ghosh *et al*., 2004), the assembly and stability of invadopods (Yamaguchi *et al*., 2005), and the invasion and metastasis of breast cancer cells (Wang *et al*., 2006). Our results show that mutant B-RAF controlled cofilin phosphorylation. Because cofilin regulates focal adhesions (Sumi *et al*., 1999; Dang *et al*., 2006), it is likely to contribute, at least in part, to altered focal adhesion dynamics after B-RAF knockdown.

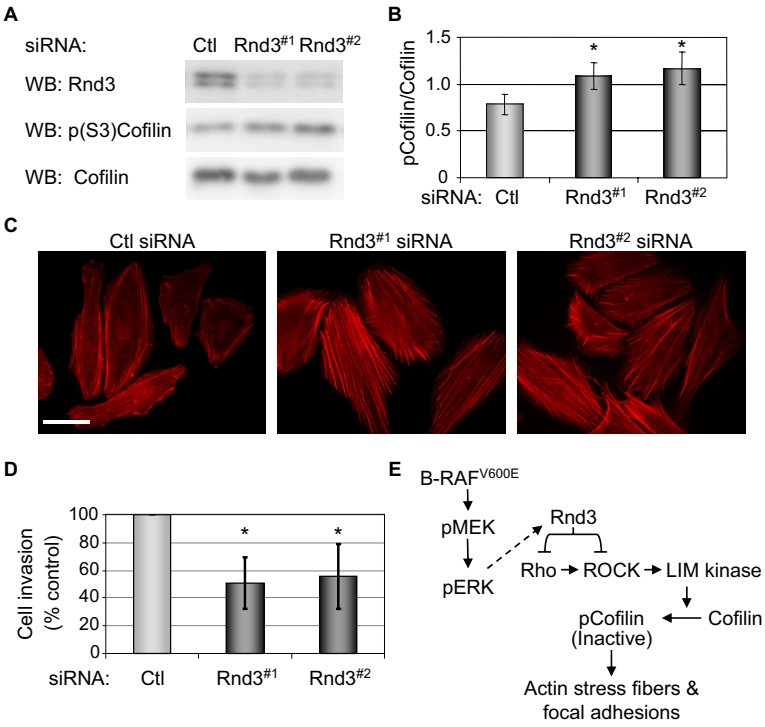

Figure 9. Rnd3 knockdown regulates the actin cytoskeleton and invasion in melanoma cells. WM793 cells were transfected with control or Rnd3 (Rnd3$^{\#1}$ or Rnd3$^{\#2}$) siRNA. (A) Cell lysates analyzed by Western blotting for Rnd3, phospho-(S3)-cofilin, and total cofilin. (B) The graph represents the relative amounts of phospho-cofilin in melanoma cells from three independent experiments. (C) F-actin organization visualized using TRITC-conjugated phalloidin. Bars, 50 μm. (D) Twenty-four hour Matrigel cell invasion assay using WM793 cells after control or Rnd3 knockdown. Asterisks denote statistical significance as determined by a two-tailed unpaired *t* test comparing cells Rnd3 knockdowns with controls (*$p < 0.05$). (E) Model for mutant B-RAF regulation of melanoma cell invasion via cross-talk between the B-RAF/MEK/ERK and Rho/ROCK/LIM kinase/cofilin signaling pathways leading to alterations in actin cytoskeletal and focal adhesion dynamics.

Although our studies in VGP melanoma cells implicate inhibition of Rho/ROCK signaling in the suppression of actin stress fibers, we cannot rule out a requirement for enhanced Rho GTPase activity during later stages of melanoma progression. Enhanced expression of RhoC has been correlated with the metastasis of melanoma cells (Clark *et al.*, 2000), and Rho/ROCK signaling is required for the invasive activity of metastatic melanoma cells (Sahai and Marshall, 2003). Notably, in a mammary adenocarcinoma model, RhoC is dispensable for the initiation and progression of primary tumors, but it is essential for metastasis (Hakem *et al.*, 2005).

Finely balanced Rho activation regulates cell migration in part through its control of focal adhesion turnover (Webb *et al.*, 2004; Gupton and Waterman-Storer, 2006). We show that mutant B-RAF signaling regulates focal adhesions in melanoma cells. ERK1/2 activation has previously been shown to regulate focal adhesion turnover (Webb *et al.*, 2004), through its modulation of focal adhesion proteins (Fincham *et al.*, 2000; Ishibe *et al.*, 2004), proteases (Carragher *et al.*, 2003), and/or contractile machinery (Klemke *et al.*, 1997). Importantly, our data suggest that ERK regulation of Rnd3 expression is a contributing factor to focal adhesion remodeling in cells expressing mutant B-RAF.

Our studies highlight Rnd3 as a regulator of cross talk between B-RAF/MEK/ERK and the Rho/ROCK signaling pathways. We demonstrate that B-RAF is necessary in melanoma and sufficient in melanocytes to elevate Rnd3 levels. These findings corroborate and extend the previous findings that Rnd3 expression is increased in MDCK cells transformed by the expression of activated C-RAF (Hansen *et al.*, 2000) and MEK-regulated in melanoma lines (Shields *et al.*, 2007). In the latter study, Rnd3 mRNA levels were typically elevated in mutant B-RAF or N-RAS cell lines compared with melanocytes and melanoma lines that contained wild-type B-RAF/N-RAS (Shields *et al.*, 2007).

Rnd3 is largely GTP-bound within cells, due to structural alterations that lower its GTP hydrolysis rates (Foster *et al.*, 1996; Guasch *et al.*, 1998). Consequently, alterations in Rnd3 expression (Hansen *et al.*, 2000; Villalonga *et al.*, 2004; Riento *et al.*, 2005) and/or localization (Foster *et al.*, 1996; Nobes *et al.*, 1998) have been proposed to be responsible for its effects. The importance of Rnd3 expression in cancer progression is poorly understood. Rnd3 is down-regulated in prostate cancer (Bektic *et al.*, 2005), whereas it is up-regulated in pancreatic cancer (Gress *et al.*, 1996). Although in one study the expression of Rnd3 correlated with transformation (Hansen *et al.*, 2000), others have shown that Rnd3 expression inhibits Ras and C-RAF–induced transformation of NIH-3T3 cells (Villalonga *et al.*, 2004; Riento *et al.*, 2005). Furthermore, Rnd3 expression supports increased cell migration of MDCK cells (Guasch *et al.*, 1998), but it suppresses p53$^{-/-}$ MEF invasion through Matrigel (Gadea *et al.*, 2007). Together, these reports suggest that Rnd3 may have a complicated role in cell transformation, migration, and invasion.

Our results implicate mutant B-RAF control of Rnd3 in the disruption of the actin cytoskeleton and large/mature focal adhesions in melanoma. Consistent with Rnd3 acting as an antagonist of Rho/ROCK signaling, Rnd3 knockdown led to the formation of actin stress fibers, albeit not as prominent as those formed after B-RAF knockdown. Therefore, it seems likely that additional mutant B-RAF controlled mechanisms participate in the regulation of melanoma cytoskeletal organization. Nevertheless, our results implicate Rnd3 as a B-RAF target and regulator of the actin cytoskeleton and cell invasion in melanoma.

In summary, we provide the first evidence that B-RAF regulates cytoskeletal organization and focal adhesion turnover in melanoma cells. These effects are mediated through control of the Rho/ROCK/LIM kinase/cofilin pathway. Furthermore, Rnd3 acts downstream of B-RAF and serves as an important regulator of cross talk between the RAF/MEK/ERK and Rho/ROCK signaling pathways. These findings underscore the need to identify mechanisms contributing to the expression and function of Rnd3 in melanoma.

ACKNOWLEDGMENTS

We are grateful to Dr. M. Herlyn for providing melanoma cell lines. We thank Drs. K. Pumiglia, J. Settleman, R. Marais, T. Nakamura, T. Sumi, P. Caroni, B. Geiger, S. Narumiya, and P. Aspenström for providing valuable reagents. We also thank Dr. K. Boisvert-Adamo for purifying adenoviruses, Dr. G. Liu for technical assistance, and Drs. P. Higgins and P. Vincent for critically reviewing this manuscript. We appreciate The Birth Place at Albany Medical Center for providing tissue samples for melanocyte isolation. This work was supported by National Institutes of Health grant GM-067893 (to A.E.A.).

REFERENCES

Arber, S., Barbayannis, F. A., Hanser, H., Schneider, C., Stanyon, C. A., Bernard, O., and Caroni, P. (1998). Regulation of actin dynamics through phosphorylation of cofilin by LIM-kinase. Nature *393*, 805–809.

Aspenstrom, P., Fransson, A., and Saras, J. (2004). Rho GTPases have diverse effects on the organization of the actin filament system. Biochem. J. *377*, 327–337.

Balaban, N. Q. *et al*. (2001). Force and focal adhesion assembly: a close relationship studied using elastic micropatterned substrates. Nat. Cell Biol. *3*, 466–472.

Bektic, J., Pfeil, K., Berger, A. P., Ramoner, R., Pelzer, A., Schafer, G., Kofler, K., Bartsch, G., and Klocker, H. (2005). Small G-protein RhoE is underexpressed in prostate cancer and induces cell cycle arrest and apoptosis. Prostate *64*, 332–340.

Bhatt, K. V., Hu, R., Spofford, L. S., and Aplin, A. E. (2007). Mutant B-RAF signaling and cyclin D1 regulate Cks1/S-phase kinase-associated protein 2-mediated degradation of p27Kip1 in human melanoma cells. Oncogene *26*, 1056–1066.

Bhatt, K. V., Spofford, L. S., Aram, G., McMullen, M., Pumiglia, K., and Aplin, A. E. (2005). Adhesion control of cyclin D1 and p27Kip1 levels is deregulated in melanoma cells through BRAF-MEK-ERK signaling. Oncogene *12*, 3459–3471.

Boisvert-Adamo, K., and Aplin, A. E. (2006). B-RAF and PI-3 kinase signaling protect melanoma cells from anoikis. Oncogene *25*, 4848–4856.

Calipel, A., Lefevre, G., Pouponnot, C., Mouriaux, F., Eychene, A., and Mascarelli, F. (2003). Mutation of B-Raf in human choroidal melanoma cells mediates cell proliferation and transformation through the MEK/ERK pathway. J. Biol. Chem. *278*, 42409–42418.

Carragher, N. O., Westhoff, M. A., Fincham, V. J., Schaller, M. D., and Frame, M. C. (2003). A novel role for FAK as a protease-targeting adaptor protein: regulation by p42 ERK and Src. Curr. Biol. *13*, 1442–1450.

Chardin, P. (2006). Function and regulation of Rnd proteins. Nat. Rev. Mol. Cell Biol. *7*, 54–62.

Chrzanowska-Wodnicka, M., and Burridge, K. (1996). Rho-stimulated contractility drives the formation of stress fibers and focal adhesions. J. Cell Biol. *133*, 1403–1415.

Clark, E. A., Golub, T. R., Lander, E. S., and Hynes, R. O. (2000). Genomic analysis of metastasis reveals an essential role for RhoC. Nature *406*, 532–535.

Conner, S. R., Scott, G., and Aplin, A. E. (2003). Adhesion-dependent activation of the ERK1/2 cascade is by-passed in melanoma cells. J. Biol. Chem. *278*, 34548–34554.

Dang, D., Bamburg, J. R., and Ramos, D. M. (2006). Alpha V Beta 3 integrin and cofilin modulate K1735 melanoma cell invasion. Exp. Cell Res. *312*, 468–477.

Davies, H. *et al*. (2002). Mutations of the BRAF gene in human cancer. Nature *417*, 949–954.

Dong, J., Phelps, R. G., Qiao, R., Yao, S., Benard, O., Ronai, Z., and Aaronson, S. A. (2003). BRAF oncogenic mutations correlate with progression rather than initiation of human melanoma. Cancer Res. *63*, 3883–3885.

Fincham, V. J., James, M., Frame, M. C., and Winder, S. J. (2000). Active ERK/MAP kinase is targeted to newly forming cell-matrix adhesions by integrin engagement and v-Src. EMBO J. *19*, 2911–2923.

Foster, R., Hu, K. Q., Lu, Y., Nolan, K. M., Thissen, J., and Settleman, J. (1996). Identification of a novel human Rho protein with unusual properties: GTPase deficiency and in vivo farnesylation. Mol. Cell. Biol. *16*, 2689–2699.

Gadea, G., de Toledo, M., Anguille, C., and Roux, P. (2007). Loss of p53 promotes RhoA-ROCK-dependent cell migration and invasion in 3D matrices. J. Cell Biol. *178*, 23–30.

Ghosh, M., Song, X., Mouneimne, G., Sidani, M., Lawrence, D. S., and Condeelis, J. S. (2004). Cofilin promotes actin polymerization and defines the direction of cell motility. Science *304*, 743–746.

Gress, T. M., Muller-Pillasch, F., Geng, M., Zimmerhackl, F., Zehetner, G., Friess, H., Buchler, M., Adler, G., and Lehrach, H. (1996). A pancreatic cancer-specific expression profile. Oncogene *13*, 1819–1830.

Guasch, R. M., Scambler, P., Jones, G. E., and Ridley, A. J. (1998). RhoE regulates actin cytoskeleton organization and cell migration. Mol. Cell. Biol. *18*, 4761–4771.

Gupton, S. L., and Waterman-Storer, C. M. (2006). Spatiotemporal feedback between actomyosin and focal-adhesion systems optimizes rapid cell migration. Cell *125*, 1361–1374.

Hakem, A., Sanchez-Sweatman, O., You-Ten, A., Duncan, G., Wakeham, A., Khokha, R., and Mak, T. W. (2005). RhoC is dispensable for embryogenesis and tumor initiation but essential for metastasis. Genes Dev. *19*, 1974–1979.

Hansen, S. H., Zegers, M.M.P., Woodrow, M., Rodriguez-Viciana, P., Chardin, P., Mostov, K. E., and McMahon, M. (2000). Induced expression of Rnd3 is associated with transformation of polarized epithelial cells by the Raf-MEK-extracellular signal-regulated kinase pathway. Mol. Cell. Biol. *20*, 9364–9375.

Hingorani, S. R., Jacobetz, M. A., Robertson, G. P., Herlyn, M., and Tuveson, D. A. (2003). Suppression of BRAF(V599E) in human melanoma abrogates transformation. Cancer Res. *63*, 5198–5202.

Huntington, J. T., Shields, J. M., Der, C. J., Wyatt, C. A., Benbow, U., Slingluff, C. L., Jr., and Brinckerhoff, C. E. (2004). Overexpression of collagenase 1 (MMP-1) is mediated by the ERK pathway in invasive melanoma cells: role of BRAF mutation and fibroblast growth factor signaling. J. Biol. Chem. *279*, 33168–33176.

Huser, M., Luckett, J., Chiloeches, A., Mercer, K., Iwobi, M., Giblett, S., Sun, X. M., Brown, J., Marais, R., and Pritchard, C. (2001). MEK kinase activity is not necessary for Raf-1 function. EMBO J. *20*, 1940–1951.

Ishibe, S., Joly, D., Liu, Z.-X., and Cantley, L. G. (2004). Paxillin serves as an ERK-regulated scaffold for coordinating FAK and Rac activation in epithelial morphogenesis. Mol. Cell *16*, 257–267.

Jaffe, A. B., and Hall, A. (2005). Rho GTPases: biochemistry and biology. Annu. Rev. Cell Dev. Biol. *21*, 247–269.

Kimura, E. T., Nikiforova, M. N., Zhu, Z., Knauf, J. A., Nikiforov, Y. E., and Fagin, J. A. (2003). High prevalence of BRAF mutations in thyroid cancer: genetic evidence for constitutive activation of the RET/PTC-RAS-BRAF signaling pathway in papillary thyroid carcinoma. Cancer Res. *63*, 1454–1457.

Kimura, K. *et al*. (1996). Regulation of myosin phosphatase by Rho and Rho-associated kinase (Rho-kinase). Science *273*, 245–248.

Klemke, R. L., Cai, S., Giannini, A. L., Gallagher, P. J., de Lanerolle, P., and Cheresh, D. A. (1997). Regulation of cell motility by mitogen-activated protein kinase. J. Cell Biol. *137*, 481–492.

Maekawa, M., Ishizaki, T., Boku, S., Watanabe, N., Fujita, A., Iwamatsu, A., Obinata, T., Ohashi, K., Mizuno, K., and Narumiya, S. (1999). Signaling from Rho to the actin cytoskeleton through protein kinases ROCK and LIM-kinase. Science *285*, 895–898.

McMahon, M. (2001). Steroid receptor fusion proteins for conditional activation of Raf-MEK-ERK signaling pathway. Methods Enzymol. *332*, 401–417.

Mikula, M., Schreiber, M., Husak, Z., Kucerova, L., Ruth, J., Wieser, R., Zatloukal, K., Beug, H., Wagner, E. F., and Baccarini, M. (2001). Embryonic lethality and fetal liver apoptosis in mice lacking the c-raf-1 gene. EMBO J. *20*, 1952–1962.

Nobes, C. D., Lauritzen, I., Mattei, M. G., Paris, S., Hall, A., and Chardin, P. (1998). A new member of the Rho family, Rnd1, promotes disassembly of actin filament structures and loss of cell adhesion. J. Cell Biol. *141*, 187–197.

Ohashi, K., Hosoya, T., Takahashi, K., Hing, H., and Mizuno, K. (2000a). A *Drosophila* homolog of LIM-kinase phosphorylates cofilin and induces actin cytoskeletal reorganization. Biochem. Biophys. Res. Commun. *276*, 1178–1185.

Ohashi, K., Nagata, K., Maekawa, M., Ishizaki, T., Narumiya, S., and Mizuno, K. (2000b). Rho-associated kinase ROCK activates LIM-kinase 1 by phosphorylation at threonine 508 within the activation loop. J. Biol. Chem. *275*, 3577–3582.

Ongusaha, P. P., Kim, H.-G., Boswell, S. A., Ridley, A. J., Der, C. J., Dotto, G. P., Kim, Y.-B., Aaronson, S. A., and Lee, S. W. (2006). RhoE is a pro-survival p53 target gene that inhibits ROCK I-mediated apoptosis in response to genotoxic stress. Curr. Biol. *16*, 2466–2472.

Pawlak, G., and Helfman, D. M. (2002a). MEK mediates v-Src-induced disruption of the actin cytoskeleton via Inactivation of the Rho-ROCK-LIM kinase pathway. J. Biol. Chem. *277*, 26927–26933.

Pawlak, G., and Helfman, D. M. (2002b). Post-transcriptional down-regulation of ROCKI/Rho-kinase through an MEK-dependent pathway leads to cytoskeleton disruption in Ras-transformed fibroblasts. Mol. Biol. Cell *13*, 336–347.

Pfaffl, M. W. (2001). A new mathematical model for relative quantification in real-time RT-PCR. Nucleic Acids Res. *29*, e45.

Pollock, C. B., Shirasawa, S., Sasazuki, T., Kolch, W., and Dhillon, A. S. (2005). Oncogenic K-RAS is required to maintain changes in cytoskeletal organization, adhesion, and motility in colon cancer cells. Cancer Res. *65*, 1244–1250.

Pritchard, C. A., Hayes, L., Wojnowski, L., Zimmer, A., Marais, R. M., and Norman, J. C. (2004). B-Raf acts via the ROCKII/LIMK/cofilin pathway to maintain actin stress fibers in fibroblasts. Mol. Cell. Biol. *24*, 5937–5952.

Rajagopalan, H., Bardelli, A., Lengauer, C., Kinzler, K. W., Vogelstein, B., and Velculescu, V. E. (2002). Tumorigenesis: RAF/RAS oncogenes and mismatch-repair status. Nature *418*, 934

Ren, X. D., Kiosses, W. B., and Schwartz, M. A. (1999). Regulation of the small GTP-binding protein Rho by cell adhesion and the cytoskeleton. EMBO J. *18*, 578–585.

Ridley, A. J., and Hall, A. (1992). The small GTP-binding protein rho regulates the assembly of focal adhesions and actin stress fibers in response to growth factors. Cell *70*, 389–399.

Riento, K., Guasch, R. M., Garg, R., Jin, B., and Ridley, A. J. (2003). RhoE binds to ROCK I and inhibits downstream signaling. Mol. Cell. Biol. *23*, 4219–4229.

Riento, K., Totty, N., Villalonga, P., Garg, R., Guasch, R., and Ridley, A. J. (2005). RhoE function is regulated by ROCK I-mediated phosphorylation. EMBO J. *24*, 1170–1180.

Sahai, E., and Marshall, C. J. (2003). Differing modes of tumour cell invasion have distinct requirements for Rho/ROCK signalling and extracellular proteolysis. Nat. Cell Biol. *5*, 711–719.

Sahai, E., Olson, M. F., and Marshall, C. J. (2001). Cross-talk between Ras and Rho signalling pathways in transformation favours proliferation and increased motility. EMBO J. *20*, 755–766.

Satyamoorthy, K., DeJesus, E., Linnenbach, A. J., Kraj, B., Kornreich, D. L., Rendle, S., Elder, D. E., and Herlyn, M. (1997). Melanoma cell lines from different stages of progression and their biological and molecular analyses. Melanoma Res. *7*, S35–S42.

Sekine, A., Fujiwara, M., and Narumiya, S. (1989). Asparagine residue in the Rho gene product is the modification site for botulinum ADP-ribosyltransferase. J. Biol. Chem. *264*, 8602–8605.

Sharma, A., Trivedi, N. R., Zimmerman, M. A., Tuveson, D. A., Smith, C. D., and Robertson, G. P. (2005). Mutant V599E B-Raf regulates growth and vascular development of malignant melanoma tumors. Cancer Res. *65*, 2412–2421.

Shields, J. M. *et al*. (2007). Lack of extracellular signal-regulated kinase mitogen-activated protein kinase signaling shows a new type of melanoma. Cancer Res. *67*, 1502–1512.

Sumi, T., Matsumoto, K., and Nakamura, T. (2001). Specific activation of LIM kinase 2 via phosphorylation of threonine 505 by ROCK, a Rho-dependent protein kinase. J. Biol. Chem. *276*, 670–676.

Sumi, T., Matsumoto, K., Takai, Y., and Nakamura, T. (1999). Cofilin phosphorylation and actin cytoskeletal dynamics regulated by Rho- and Cdc42-activated LIM-kinase 2. J. Cell Biol. *147*, 1519–1532.

Sumimoto, H., Miyagishi, M., Miyoshi, H., Yamagata, S., Shimizu, A., Taira, K., and Kawakami, Y. (2004). Inhibition of growth and invasive ability of melanoma by inactivation of mutated BRAF with lentivirus-mediated RNA interference. Oncogene *23*, 6031–6039.

Vial, E., Sahai, E., and Marshall, C. J. (2003). ERK-MAPK signaling coordinately regulates activity of Rac1 and RhoA for tumor cell motility. Cancer Cell *4*, 67–79.

Villalonga, P., Guasch, R. M., Riento, K., and Ridley, A. J. (2004). RhoE inhibits cell cycle progression and Ras-induced transformation. Mol. Cell. Biol. *24*, 7829–7840.

Wang, W., Mouneimne, G., Sidani, M., Wyckoff, J., Chen, X., Makris, A., Goswami, S., Bresnick, A. R., and Condeelis, J. S. (2006). The activity status of cofilin is directly related to invasion, intravasation, and metastasis of mammary tumors. J. Cell Biol. *173*, 395–404.

Watanabe, N., Kato, T., Fujita, A., Ishizaki, T., and Narumiya, S. (1999). Cooperation between mDia1 and ROCK in Rho-induced actin reorganization. Nat. Cell Biol. *1*, 136–143.

Webb, D. J., Donais, K., Whitmore, L. A., Thomas, S. M., Turner, C. E., Parsons, J. T., and Horwitz, A. F. (2004). FAK-Src signalling through paxillin, ERK and MLCK regulates adhesion disassembly. Nat. Cell Biol. *6*, 154–161.

Wellbrock, C., Ogilvie, L., Hedley, D., Karasarides, M., Martin, J., Niculescu-Duvaz, D., Springer, C. J., and Marais, R. (2004). V599E B-RAF is an oncogene in melanocytes. Cancer Res. *64*, 2338–2342.

Wennerberg, K., Forget, M.-A., Ellerbroek, S. M., Arthur, W. T., Burridge, K., Settleman, J., Der, C. J., and Hansen, S. H. (2003). Rnd proteins function as RhoA antagonists by activating p190 RhoGAP. Curr. Biol. *13*, 1106–1115.

Yamaguchi, H. *et al*. (2005). Molecular mechanisms of invadopodium formation: the role of the N-WASP-Arp2/3 complex pathway and cofilin. J. Cell Biol. *168*, 441–452.

Yang, N., Higuchi, O., Ohashi, K., Nagata, K., Wada, A., Kangawa, K., Nishida, E., and Mizuno, K. (1998). Cofilin phosphorylation by LIM-kinase 1 and its role in Rac-mediated actin reorganization. Nature *393*, 809–812.

Yoneda, A., Ushakov, D., Multhaupt, H.A.B., and Couchman, J. R. (2007). Fibronectin matrix assembly requires distinct contributions from Rho kinases I and -II. Mol. Biol. Cell *18*, 66–75.